


# Paracellular bicarbonate flux across human cystic fibrosis airway epithelia tempers changes in airway surface liquid pH

Ian M. Thornell<sup>1</sup> , Tayyab Rehman<sup>1</sup>, Alejandro A. Pezzulo<sup>1</sup> and Michael J. Welsh<sup>1,2,3</sup> 

<sup>1</sup>Department of Internal Medicine, Pappajohn Biomedical Institute, Roy J. and Lucille A. Carver College of Medicine, University of Iowa, Iowa City, IA, USA

<sup>2</sup>Department of Molecular Physiology and Biophysics, Pappajohn Biomedical Institute, Roy J. and Lucille A. Carver College of Medicine, University of Iowa, Iowa City, IA, USA

<sup>3</sup>Howard Hughes Medical Institute, University of Iowa, Iowa City, IA, USA

Edited by: Peying Fong & Rajini Rao

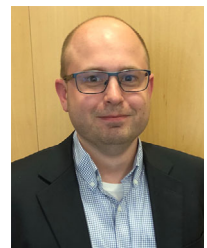
Linked articles: This article is highlighted in a Perspectives article by Parker. To read this article, visit <https://doi.org/10.1113/JP280467>.

## Key points

- $\text{Cl}^-$  and  $\text{HCO}_3^-$  had similar paracellular permeabilities in human airway epithelia.
- $P_{\text{Cl}}/P_{\text{Na}}$  of airway epithelia was unaltered by pH 7.4 vs. pH 6.0 solutions.
- Under basal conditions, calculated paracellular  $\text{HCO}_3^-$  flux was secretory.
- Cytokines that increased airway surface liquid pH decreased or reversed paracellular  $\text{HCO}_3^-$  flux.
- $\text{HCO}_3^-$  flux through the paracellular pathway may counterbalance effects of cellular  $\text{H}^+$  and  $\text{HCO}_3^-$  secretion.

**Abstract** Airway epithelia control the pH of airway surface liquid (ASL), thereby optimizing respiratory defences. Active  $\text{H}^+$  and  $\text{HCO}_3^-$  secretion by airway epithelial cells produce an ASL that is acidic compared with the interstitial space. The paracellular pathway could provide a route for passive  $\text{HCO}_3^-$  flux that also modifies ASL pH. However, there is limited information about paracellular  $\text{HCO}_3^-$  flux, and it remains uncertain whether an acidic pH produced by loss of cystic fibrosis transmembrane conductance regulator anion channels or proinflammatory cytokines might alter the paracellular pathway function. To investigate paracellular  $\text{HCO}_3^-$  transport, we studied differentiated primary cultures of human cystic fibrosis (CF) and non-CF airway epithelia. The paracellular pathway was pH-insensitive at pH 6.0 vs. pH 7.4 and was equally permeable to  $\text{Cl}^-$  and  $\text{HCO}_3^-$ . Under basal conditions at pH  $\sim$ 6.6, calculated paracellular  $\text{HCO}_3^-$  flux was weakly secretory. Treating epithelia with IL-17 plus  $\text{TNF}\alpha$  alkalinized ASL pH to  $\sim$ 7.0, increased paracellular  $\text{HCO}_3^-$  permeability, and paracellular  $\text{HCO}_3^-$  flux was negligible. Applying IL-13

**Ian Thornell** is a Research Assistant Professor of Internal Medicine at the University of Iowa. He trained in ion transport and pH physiology as a graduate student with Mark Bevensee (University of Alabama Birmingham) and as a postdoctoral scholar with Michael Welsh (Howard Hughes Medical Institute and University of Iowa). His lab investigates how transepithelial transport influences physiology and disease using a combination of molecular biology and genetic techniques, animal models, electrophysiology, and optical methods.



increased ASL pH to  $\sim 7.4$  without altering paracellular  $\text{HCO}_3^-$  permeability, and calculated paracellular  $\text{HCO}_3^-$  flux was absorptive. These results suggest that  $\text{HCO}_3^-$  flux through the paracellular pathway counterbalances, in part, changes in the ASL pH produced via cellular mechanisms. As the pH of ASL increases towards that of basolateral liquid, paracellular  $\text{HCO}_3^-$  flux becomes absorptive, tempering the alkaline pH generated by transcellular  $\text{HCO}_3^-$  secretion.

(Received 6 May 2020; accepted after revision 22 June 2020; first published online 5 July 2020)

**Correspondence author** I. M. Thornell: Department of Internal Medicine, Iowa City, IA 52242 USA. Email: ian-thornell@uiowa.edu

M. J. Welsh: Department of Internal Medicine, Iowa City, IA 52242 USA. Email: michael-welsh@uiowa.edu

## Introduction

The acid-base status of airway surface liquid (ASL) is tightly regulated (Fischer & Widdicombe, 2006). Active proton secretion produces an ASL pH that is acidic compared with the interstitial space (Jayaraman *et al.* 2001a; Coakley *et al.* 2003; McShane *et al.* 2003; Pezzulo *et al.* 2012; Garland *et al.* 2013; Abou Alaiwa *et al.* 2014a; Schultz *et al.* 2017; Abou Alaiwa *et al.* 2018).  $\text{H}^+$  secretion is neutralized, in part, by  $\text{HCO}_3^-$  secretion by the cystic fibrosis transmembrane conductance regulator (CFTR) anion channel,  $\text{Ca}^{2+}$ -activated  $\text{Cl}^-$  channels, and pendrin-mediated  $\text{Cl}^-/\text{HCO}_3^-$  exchange (Coakley *et al.* 2003; Fischer & Widdicombe, 2006; Shah *et al.* 2016; Lennox *et al.* 2018; Simonin *et al.* 2019). In cystic fibrosis (CF), loss of CFTR-mediated  $\text{HCO}_3^-$  secretion decreases the ASL pH (Pezzulo *et al.* 2012; Garland *et al.* 2013; Abou Alaiwa *et al.* 2014a; Garnett *et al.* 2016; Haggie *et al.* 2016; Shah *et al.* 2016; Abou Alaiwa *et al.* 2018; Simonin *et al.* 2019). The acidic ASL pH impairs at least two host-defence mechanisms: antimicrobial activity (Pezzulo *et al.* 2012; Abou Alaiwa *et al.* 2014b; Shah *et al.* 2016; Simonin *et al.* 2019) and mucociliary transport (Clary-Meinesz *et al.* 1998; Hoegger *et al.* 2014; Tang *et al.* 2016; Ostedgaard *et al.* 2017).

In parallel with the cellular pathway, with its channels, transporters and pumps, lies the paracellular pathway, which allows passive ion flux (Diamond, 1978; Anderson & Van Itallie, 2009). The paracellular pathway could provide a route for  $\text{HCO}_3^-$  secretion or absorption, and thus it could modify ASL pH. However,  $\text{HCO}_3^-$  flux through the paracellular pathway is rarely considered, perhaps because the use of the short-circuit technique negates the influence of the paracellular pathway.

$\text{HCO}_3^-$  flux through the paracellular pathway might perturb ASL pH in disease. As an example, the ASL of newborn humans with CF, newborn CF pigs, and differentiated cultures of human and pig CF airway epithelia is more acidic than non-CF ASL (Coakley *et al.* 2003; Pezzulo *et al.* 2012; Garland *et al.* 2013; Abou Alaiwa *et al.* 2014a; Garnett *et al.* 2016; Haggie *et al.* 2016; Shah *et al.* 2016; Abou Alaiwa *et al.* 2018; Simonin *et al.* 2019). However, over the course of months and years, the *in vivo* pH of CF ASL alkalinizes (Abou

Alaiwa *et al.* 2014a; Schultz *et al.* 2017; Abou Alaiwa *et al.* 2018). These findings suggest that an *in vivo* factor might contribute to age-dependent alkalinization. Airway inflammation develops over a similar time course (Khan *et al.* 1995; Muhlebach *et al.* 1999; Dakin *et al.* 2002; Sly *et al.* 2009). Consistent with the hypothesis that inflammation may increase ASL pH, previous reports suggest that proinflammatory cytokines alter ASL pH in primary cultures of CF epithelia (Kreindler *et al.* 2009; Gorrieri *et al.* 2016; Haggie *et al.* 2016; Lennox *et al.* 2018; Scudieri *et al.* 2018; Kim *et al.* 2019; Rehman *et al.* 2020).

Thus, further knowledge of the  $\text{HCO}_3^-$  permeability and flux via the paracellular pathway could aid understanding of how ASL pH is controlled. To assess paracellular  $\text{HCO}_3^-$  permeability, we first tested whether pH alters the paracellular permeability of airway epithelia. We then evaluated the paracellular  $\text{HCO}_3^-$  permeability and calculated the paracellular  $\text{HCO}_3^-$  flux in the absence and presence of cytokines that are associated with airway inflammation.

## Methods

Airway epithelial cells were obtained from CF and non-CF tissue obtained from the Iowa Donor Network with CF donor information supplied in Table 1 and studies were approved by the University of Iowa Institutional Review Board and conform to the principles and regulations of *The Journal of Physiology* (Grundy, 2015). Epithelial cells were cultured according to a previous protocol (Karp *et al.* 2002). Briefly, donor tissue was digested with pronase then seeded upon collagen-coated semi-permeable membranes (0.33  $\text{cm}^2$  polycarbonate filters, Costar #3413) and grown at an air-liquid interface. Cultures were used after complete cellular differentiation (>21 days) and resistances >166  $\Omega \cdot \text{cm}^2$ .

## Solutions

All chemicals were from Sigma-Aldrich unless otherwise stated. All dilution potential solutions consisted of the same minor salts and glucose in mM; 5 glucose, 1.2 calcium gluconate, 1.2 magnesium gluconate, and were buffered with 5 Hepes (pH 7.4 solutions) or 5 MES (pH 6.0

**Table 1. Cystic fibrosis donors used in this study**

Donor	Age	Sex	Cystic fibrosis transmembrane conductance regulator mutations
1	27	Female	ΔF508/1717-1G>A
2	36	Female	ΔF508/R347P
3	29	Female	ΔF508/3876delA
4	36	Female	ΔF508/ΔF508
5	22	Male	ΔF508/1717-1G-A
6	21	Female	ΔF508/2622 + 1G>A
7	36	Male	ΔF508/R553X
8	64	Male	ΔF508/L1254X
9	37	Male	ΔF508/deletions of exons 2–3
10	38	Male	ΔF508/ΔF508
11	19	Female	ΔF508/G85E
12	31	Female	ΔF508/ΔF508
13	24	Female	ΔF508/unknown
14	31	Female	ΔF508/G551D
15	42	Female	ΔF508/ΔF508
16	34	Female	ΔF508/3659delC
17	54	Female	ΔF508/I336K
18	35	Female	ΔF508/2184insA
19	24	Female	ΔF508/G551D
20	29	Female	ΔF508/3849 + 10kbC→T

solutions) and titrated at 37°C to their respective pH value with N-methyl-D-glucamine (NMDG), a cell- and junctional-impermeant sugar, that acts as a strong base (i.e. >99% dissociation) at pH 7.4 and 6.0 (pKa 9.6; 22°C). The [NMDG<sup>+</sup>] added was < 1 mM and was therefore excluded from ionic strength calculations. All major salts (e.g. NaCl) were made at the following concentrations in mM; 150, 112.5, 75, 37.5 or 18.75 and were gassed with compressed air. All solutions were made to 310 ± 5 mOsm by mannitol addition and verified by a vapour pressure osmometer (Wescor Inc.) each time a solution was made. Solutions were made on the day of each experiment.

For solutions containing HCO<sub>3</sub><sup>-</sup>, the [HCO<sub>3</sub><sup>-</sup>] was computed using the Henderson–Hasselbalch equation. 5% CO<sub>2</sub> partial pressure was calculated using the average atmospheric pressure of Iowa City (765.5 mmHg; Iowa City Municipal Airport) and correcting for the vapour pressure of water (47.10 mmHg). For dilution potential experiments, NaHCO<sub>3</sub> and respective NaCl control solutions were (in mM) 22 or 11. The basolateral solution was 22 mM NaHCO<sub>3</sub> or 22 mM NaCl for their respective experiments. The NaCl control solution for NaHCO<sub>3</sub> experiments was titrated to the same pH value as its corresponding NaHCO<sub>3</sub> solution to control for possible pH-dependent effects. Calculated pH values for these experiments were pH 7.4 and pH 7.1. However, empirical pH values for these NaHCO<sub>3</sub> solutions equilibrated with

5% CO<sub>2</sub> were 7.58 (22 mM NaHCO<sub>3</sub>) and 7.21 (11 mM HCO<sub>3</sub><sup>-</sup>), which may be attributed to the increased pKa of HCO<sub>3</sub><sup>-</sup> (Hastings & Sendroy, 1925) and decreased CO<sub>2</sub> solubility (Van Slyke *et al.* 1928) for low ionic strength solutions. Therefore, control NaCl solutions were titrated to these empirical pH values with NMDG. The paracellular NaCl permeability for pH 7.58 or pH 7.21 low ionic strength experiments did not differ from values obtained from pH 7.4 or pH 6.0 experiments performed at higher ionic strengths. All NaHCO<sub>3</sub> solutions were gassed with 5% CO<sub>2</sub>/21%O<sub>2</sub> balanced with nitrogen and all NaCl solutions were gassed with air.

For open-circuit experiments performed to estimate paracellular HCO<sub>3</sub><sup>-</sup> current, three different solutions were used. The basolateral solution contained in mM: 5 glucose, 104.8 sodium chloride, 22 sodium bicarbonate, 5.2 potassium chloride, 18.2 sodium gluconate, 1.2 calcium gluconate, 1.2 magnesium gluconate, 2.2 NMDG and 2.2 gluconic acid. Physiological ASL solutions contained 5 glucose, 70 sodium chloride, 20 potassium chloride, 1.2 calcium gluconate, 1.2 magnesium gluconate, 26.3 NMDG, 26.3 gluconic acid and either 22 sodium bicarbonate/13 sodium gluconate (pH 7.4) or 4 sodium bicarbonate/31 sodium gluconate (pH 6.6). These solutions approximate the ionic activity of native human ASL cultured at the air–liquid interface (Knowles *et al.* 1997; Jayaraman *et al.* 2001b; Namkung *et al.* 2009).

### Pharmacological reagents

The following drugs and final concentrations were used in this study: 100 μM amiloride (Sigma-Aldrich), 100 μM DIDS (Sigma-Aldrich), 100 μM GlyH-101 (Cystic Fibrosis Foundation Therapeutics and Robert Bridges), and 1 mM acetazolamide (Sigma-Aldrich). All drugs were dissolved in DMSO (Thermo Fisher Scientific).

### Cytokine treatment

For the cytokine studies, the media was changed every 2 days. For the IL-13 experiments, 20 ng/ml IL-13 (R&D Systems) or DMSO vehicle was added to the basolateral compartment of differentiated epithelia, then 20 μl of the basolateral solution was added to the apical surface and experiments were performed 21 days after initial treatment. 20 ng/ml IL-13 is sufficient to increase goblet cell abundance in many laboratories (Laoukili *et al.* 2001; Atherton *et al.* 2003; Zhen *et al.* 2007; Kanoh *et al.* 2011; Thavagnanam *et al.* 2011; Dickinson *et al.* 2016; Pezzulo *et al.* 2019). For IL-17/TNFα experiments, 20 ng/ml IL-17 (R&D Systems) and 10 ng/ml TNFα (R&D Systems) or DMSO was added to the basolateral media and experiments were performed 2 days later based on preliminary dose–response studies and previous reports

(Kao *et al.* 2004; McAllister *et al.* 2005; Kreindler *et al.* 2009; Choy *et al.* 2015; Lehmann *et al.* 2018; Pezzulo *et al.* 2019).

## Electrophysiology

Epithelia were assayed in Ussing chambers (Physiologic Instruments) with 3 M KCl agar bridges connected to amplifiers (VCC-MC8, Physiologic Instruments) recording open-circuit transepithelial voltage ( $V_t$ ). A 5  $\mu$ A bipolar current pulse was applied across the epithelium periodically. The current-induced change in  $V_t$  was used to calculate the transepithelial conductance ( $G_t$ ). Data were acquired with Acquire & Analyse software (version 2.3.8, Physiologic Instruments). Dilution potentials were generated by perfusing dilutions of the dominant ionic species (e.g. NaCl) into the apical chamber. After the experiment, cells were lysed by distilled water and electrode drift was assessed in the original bilateral solution. Junction potentials induced in the voltage probes by ionic dilutions were then assessed without an epithelium and subtracted from the obtained dilution potentials.

## Calculations

Activity coefficients were calculated using the ionic strength of each solution and the extended Debye–Hückel equation (Robinson & Stokes, 1959), which is applicable for physiological concentrations:

$$\log \gamma = \frac{-0.509z^2\sqrt{\mu}}{1 + 3.29\alpha\sqrt{\mu}} \quad (1)$$

Where  $\gamma$  is the activity coefficient of the ion,  $z$  is the ionic charge,  $\mu$  is the ionic strength of the solution, and  $\alpha$  is the effective diameter of the hydrated ion taken from Keilland (1937). The constants  $-0.509$  and  $3.29$  were used because experiments were performed at  $37^\circ\text{C}$  (Manov *et al.* 1943).

Ion activity was calculated by the equation:

$$a_{ion} = \gamma \times [c] \quad (2)$$

Where  $a$  is the ion activity,  $\gamma$  is the activity coefficient, and  $[c]$  is the ion concentration.

Relative permeability ( $P_{Anion}/P_{Na}$ ) was calculated using the Goldman–Hodgkin–Katz equation (Goldman, 1943; Hodgkin & Katz, 1949):

$$\Delta V_t = \frac{RT}{F} \ln \left( \frac{\alpha_{Na^+_{basolateral}} + P_{A^-/Na^+} \times \alpha_{A^-_{apical}}}{\alpha_{Na^+_{apical}} + P_{A^-/Na^+} \times \alpha_{A^-_{basolateral}}} \right) \quad (3)$$

Approximating the constants at  $37^\circ\text{C}$  simplifies to:

$$\Delta V_t = 61.5 \log \left( \frac{\alpha_{Na^+_{basolateral}} + P_{A^-/Na^+} \times \alpha_{A^-_{apical}}}{\alpha_{Na^+_{apical}} + P_{A^-/Na^+} \times \alpha_{A^-_{basolateral}}} \right) \quad (4)$$

Where  $F$  is Faraday's constant,  $R$  is the gas constant,  $T$  is temperature,  $\Delta V_t$  is the dilution potential,  $a$  is the ionic activity, and  $P_{A^-/Na^+}$  is the relative permeability of anion  $A^-$  to  $Na^+$ . When bi-ionic potentials were measured (potential generated by replacing apical NaCl with an equimolar monovalent chloride salt), we used Eqn 4 and substituted  $\alpha_{Na^+_{apical}}$  with  $P_{C^+/Na^+} \times$  the substituted cation's activity.

Partial conductance ( $G_{ion}$ ) was computed using the following formula (Schultz, 1980; Sten-Knudsen, 2002):

$$\Delta V_t = \left( \frac{G_{Na}}{G_p} \times E_{Na} \right) + \left( \frac{G_p - G_{Na}}{G_p} \times E_{anion} \right) \quad (5)$$

Where  $\Delta V_t$  is the dilution potential,  $G_p$  is the paracellular conductance in the corresponding symmetrical salt solution, and  $E_{Na}$  and  $E_{anion}$  are the computed Nernst potential for the ion during dilution. The value  $G_p - G_{Na}$  is the partial conductance of the anion ( $G_{anion}$ ). The quantities  $\frac{G_{Na}}{G_p}$  and  $\frac{G_p - G_{Na}}{G_p}$  represent the transference numbers for  $Na^+$  and its corresponding anion.

Absolute paracellular permeabilities were calculated using the following equation (Schultz, 1980; Sten-Knudsen, 2002):

$$P_{ion} = \tilde{G}_{ion} \frac{RT \left( 1 - e^{zFV_t/RT} \right) (V_t - E_{ion})}{(zF)^2 V_t [a_{basolateral} - a_{apical} e^{zFV_t/RT}]} \quad (6)$$

Where  $P_{ion}$  is the ion's absolute permeability,  $G_{ion}$  is the ion's partial conductance,  $z$  is the ion's charge,  $a$  is the ion's activity,  $F$  is Faraday's constant,  $R$  is the gas constant,  $T$  is temperature,  $V_t$  is the transepithelial voltage and  $E_{ion}$  is the ion's Nernst potential. We obtained similar values for  $P_{ion}$  using the approach taken by Kimizuka and Koketsu (Kimizuka & Koketsu, 1964), using total  $G$  rather than  $G_{ion}$  (not shown).

Ionic mobilities ( $\mu$ ) at  $37^\circ\text{C}$  were derived from reported limiting equivalent conductivities ( $\lambda$ ) at  $35^\circ\text{C}$  (Robinson & Stokes, 1959) by the relationship:

$$\lambda_{35^\circ\text{C}}^\circ = |z| \times \mu \times F \quad (7)$$

Where  $z$  is the ion's charge and  $F$  is Faraday's constant. A  $\mu_{\text{HCO}_3}$  of  $4.11 \times 10^{-4} \text{ cm}^2 \text{ sec}^{-1} \text{ V}^{-1}$  was derived by the Nernst–Einstein relationship:

$$\lambda_{\text{HCO}_3, 35^\circ\text{C}}^\circ = D_{\text{HCO}_3, 35^\circ\text{C}} \frac{z^2 F^2}{RT} \quad (8)$$

Where  $z$  is the ion's charge,  $F$  is Faraday's constant, and  $D$  is the  $\text{HCO}_3^-$  diffusion coefficient at  $35^\circ\text{C}$ ,  $1.10 \times 10^{-5} \text{ cm}^2 \text{ s}^{-1}$  (Voipio, 1998). We then substitute  $\lambda_{\text{HCO}_3, 35^\circ\text{C}}^\circ$  into Eqn 7 to obtain  $\mu_{\text{HCO}_3}$ .

Ionic conductance  $G_{\text{HCO}_3}$  for non-symmetrical solutions were obtained by using estimated  $P_{ion}$  values, known ionic concentrations, calculated Nernst



potentials, and empirical transepithelial voltages substituted into Eqn 6. To estimate  $P_{ion}$  for a given paracellular conductance, we used the relationship between donor-matched  $P_{HCO_3}$  estimated from 22 mM NaHCO<sub>3</sub> vs. conductance in 150 mM NaCl solution.

With the solved  $G_{ion}$ , the ion-specific current ( $I_{ion}$ ) was calculated using the driving-force derivation of Ohm's law:

$$I_{ion} = G_{ion}(V_t - E_{ion}) \quad (9)$$

Ion-specific current was transformed to ion-specific fluxes using Faraday's constant and were scaled to hours.

Paracellular flux is directly related to paracellular current by  $I_{Paracellular} = zFJ_{Paracellular}$ . Therefore, we use the term paracellular flux and paracellular current interchangeably. For the discussion, we refer to the ion concentration, [HCO<sub>3</sub><sup>-</sup>], and ion activity,  $\alpha_{HCO_3^-}$ , interchangeably. Ion activities were used for all calculations.

### Data analysis

Electrophysiological data were analysed using a custom graphical user interface coded in MATLAB version R2018b (Mathworks). Equations were solved in MATLAB version R2018b (Mathworks) using custom code. All codes were written by Ian M. Thornell and are freely available upon request and the data that support the findings of this study are available from the corresponding authors upon reasonable request.

### Statistics

An initial  $P_{Cl/Na}$  experiment ( $n = 8$  donors) was performed and data were used to perform an *a priori* power analysis for the remainder of the study using GraphPad Prism 7.0d (GraphPad) and G\*Power 3.1 software (Faul *et al.* 2007). For this initial experiment, relative permeabilities were normally distributed (the Shapiro–Wilk test) and had equal variance (F test). For the obtained effect size ( $d = 1.64$ ), six donors were used in subsequent experiments to detect a 0.1 change in relative permeability ( $\alpha = 0.05$ ,  $\beta > 0.80$ ). Data were compared using either a paired Student's *t* test, a one-way ANOVA with Bonferroni correction, or a Wilcoxon matched-pairs signed rank test. Linear fits were obtained using the least-squares method and compared using an extra sum-of-squares F test. For all tests, statistical significance was defined as  $P \leq 0.05$ . Any outliers were identified by a Grubb's test,  $\alpha \leq 0.01$ .

## Results

### Paracellular ion permeability is pH-insensitive

It is unknown whether physiological changes in apical pH alter the paracellular permeability of airway epithelia.

To evaluate paracellular permeability, we first eliminated electrogenic transcellular Na<sup>+</sup> transport by adding 100  $\mu$ M amiloride to the apical solution (Fig. 1A). To eliminate electrogenic transcellular Cl<sup>-</sup> transport, we used CF epithelia to eliminate CFTR anion channels and added 100  $\mu$ M DIDS to the apical solution to inhibit Ca<sup>+</sup>-activated Cl<sup>-</sup> channels (Ousingsawat *et al.* 2009). This combination resulted in a small apical-positive transepithelial voltage ( $V_t$ ), consistent with a previous study (Coakley *et al.* 2003). We then determined the relative paracellular Cl<sup>-</sup> to Na<sup>+</sup> permeability ( $P_{Cl/Na}$ ) by measuring changes in  $V_t$  in response to a series of apical NaCl dilutions. We set pH to 7.4 or 6.0 bilaterally; the pH buffer was Hepes or MES. At both pH 7.4 and 6.0, apical NaCl dilutions depolarized  $V_t$ , indicating that Na<sup>+</sup> was more permeable than Cl<sup>-</sup> through the paracellular pathway (Fig 1A and B).  $P_{Cl/Na}$  was not altered at pH 6.0 (Fig. 1C) suggesting that physiological pH does not alter the paracellular ion permeability of airway epithelia. We also estimated the paracellular electrical conductance ( $G_p$ ) after adding amiloride and DIDS to CF epithelia and before the measurement of dilution potentials.  $G_p$  was not affected by the changes in pH (Fig. 1D). By comparing epithelia from different donors, we found that  $P_{Cl/Na}$  was independent of  $G_p$  (Fig. 1E), and  $P_{Na}$  and  $P_{Cl}$  increased in parallel with  $G_p$  (Fig. 1F). These data suggest that epithelia with low and high  $G_p$  contain similar paracellular permeation pathways.

### Paracellular HCO<sub>3</sub><sup>-</sup> permeability is similar to paracellular Cl<sup>-</sup> permeability

Because  $P_{Cl/Na}$  was unaffected by changing from pH 7.4 to pH 6.0 solutions, we were able to assess paracellular HCO<sub>3</sub><sup>-</sup> permeability with dilution potentials, which at a constant CO<sub>2</sub> concentration will impose a concomitant pH change. Decreasing NaHCO<sub>3</sub> from 22 mM to 11 mM revealed relative HCO<sub>3</sub><sup>-</sup> permeabilities,  $P_{HCO_3/Na}$ , that were similar to pH-matched reductions in NaCl from 22 mM to 11 mM,  $P_{Cl/Na}$  (Fig. 2A). Paracellular HCO<sub>3</sub><sup>-</sup> permeability was unaffected by inhibiting carbonic anhydrase with 1 mM acetazolamide, indicating that HCO<sub>3</sub><sup>-</sup> permeated as an ion rather than carbonic anhydrase-mediated CO<sub>2</sub> reconversion reactions (Fig. 2B).

To further assess paracellular ion permeability, we tested several monovalent ions of different size. Cations were more permeant than anions (Fig. 2C). However, ionic size had minimal effects on permeation. Thus, the paracellular pathway was more selective for charge vs. ion size.

Paracellular Cl<sup>-</sup> and HCO<sub>3</sub><sup>-</sup> fluxes are determined by  $P_{Cl}$  and  $P_{HCO_3}$ , the [Cl<sup>-</sup>] and [HCO<sub>3</sub><sup>-</sup>], and  $V_t$ . To obtain the data necessary for calculating paracellular HCO<sub>3</sub><sup>-</sup> flux, open-circuit  $V_t$  and  $G_t$  were recorded from human CF and non-CF epithelia. Figure 3A shows the

sequence of additions and timing in a non-CF epithelium. The relationships between  $P_{\text{Cl}}$  and  $P_{\text{HCO}_3}$  and  $G_p$  are shown in Fig. 3B and C. Epithelia were bathed in solutions with an ASL-like composition (Knowles *et al.* 1997; Jayaraman *et al.* 2001b; Namkung *et al.* 2009) titrated to pH 6.6 and also to 7.4. For epithelia from each donor, we determined  $P_{\text{Cl}}$  and  $P_{\text{HCO}_3}$  (Fig. 3D and G). The paracellular permeabilities of these two anions were similar. We then used Eqn 6 to calculate the

paracellular  $\text{Cl}^-$  and  $\text{HCO}_3^-$  conductances for CF and non-CF epithelia (Fig. 3E and H). Because the  $[\text{HCO}_3^-]$  was less than the  $[\text{Cl}^-]$ , the paracellular conductance for  $\text{HCO}_3^-$  was less than for  $\text{Cl}^-$ . Raising the apical  $[\text{HCO}_3^-]$  increased the paracellular  $\text{HCO}_3^-$  conductance.

We also calculated the paracellular  $\text{Cl}^-$  and  $\text{HCO}_3^-$  fluxes from the driving-force derivation of Ohm's law (Eqn 9) and Faraday's constant (Fig. 3F and I). These calculations yielded two main observations. First, the

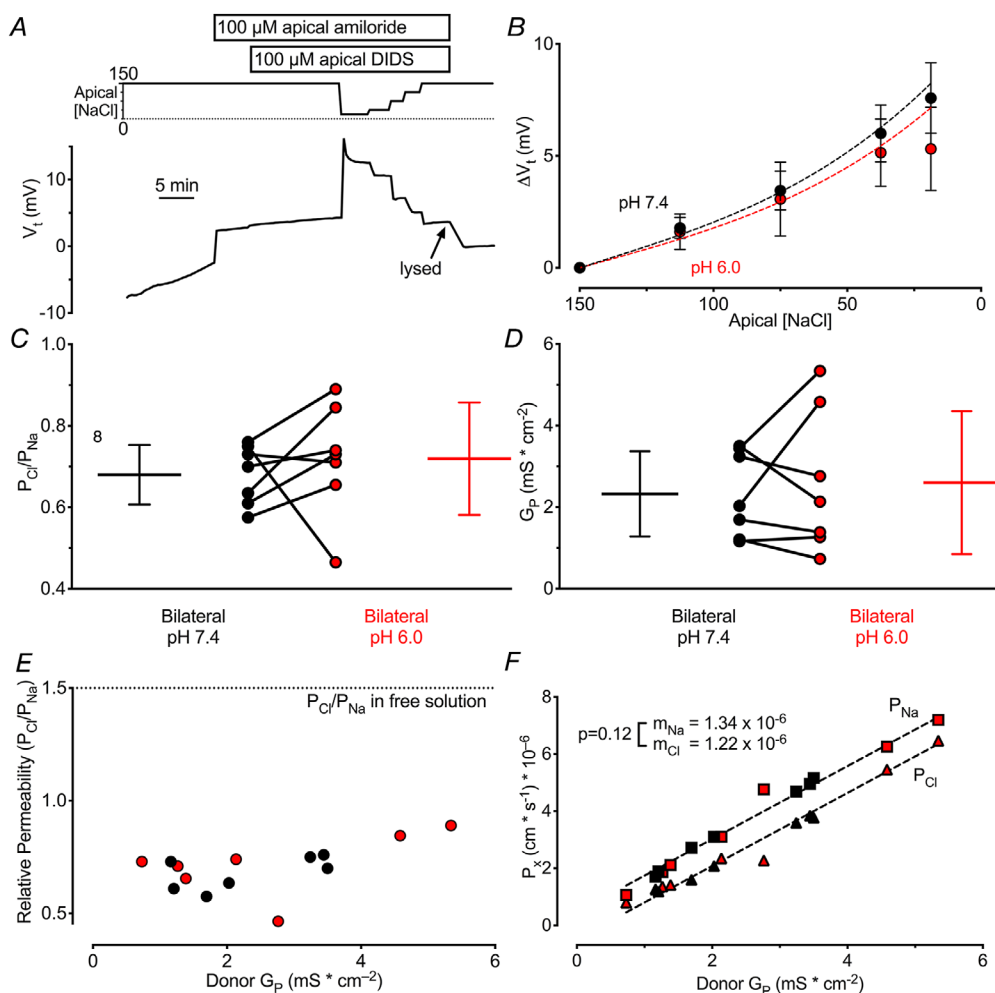


**Figure 1. Human airway epithelia cultured at the air–liquid interface have cation-selective tight junctions that are not affected by low physiological pH**

Red is pH 6.0, black is pH 7.4, squares are  $\text{Na}^+$  data and triangles are  $\text{Cl}^-$  and all error bars represent standard deviations of the mean. One donor was omitted because a  $11.43 \text{ mS cm}^{-2}$  baseline conductance was identified as an outlier; Grubb's test  $\alpha \leq 0.01$ . A, representative dilution potential experiment not corrected for junction potentials. B, junction potential-corrected dilution potential summary data for experiments containing identical solutions titrated to pH 7.4 or 6.0;  $n = 7$  donors. The dashed lines represent theoretical dilution potentials calculated by substituting average relative permeability data from panel C into the Goldman–Hodgkin–Katz equation. C, relative paracellular permeability, each circle represents a single human donor.  $P = 0.54$ ; two-tailed paired Student's  $t$  test;  $n = 7$  donors. D, bilateral 150 mM NaCl paracellular conductance. Each circle represents a single human donor.  $P = 0.63$ ; paired Student's  $t$  test;  $n = 7$  donors. E, relative paracellular permeability vs. paracellular conductance, each circle represents a single human donor. We cannot reject the null hypothesis that the slopes were zero; pH 7.4  $P = 0.15$ , pH 6.0  $P = 0.25$ ; F test;  $n = 7$  donors each. F, paracellular ion permeability vs. paracellular conductance. Data were fit with linear regressions,  $r^2 > 0.98$ . We cannot reject the null hypothesis that the slopes were equal;  $P = 0.12$ ; F test;  $n = 7$  donors each ion and pH value.

paracellular  $\text{HCO}_3^-$  flux was smaller in magnitude than the paracellular  $\text{Cl}^-$  flux. Second, for an apical pH of 6.6, the calculated paracellular fluxes were absorptive for  $\text{Cl}^-$  and slightly secretory for  $\text{HCO}_3^-$ . When we raised the apical pH to 7.4, the calculated  $\text{HCO}_3^-$  flux became absorptive. Thus, at an apical pH of 7.4, the calculated paracellular  $\text{Cl}^-$  and  $\text{HCO}_3^-$  fluxes were in the opposite direction of active transcellular  $\text{Cl}^-$  and  $\text{HCO}_3^-$  secretion observed for airway epithelia.

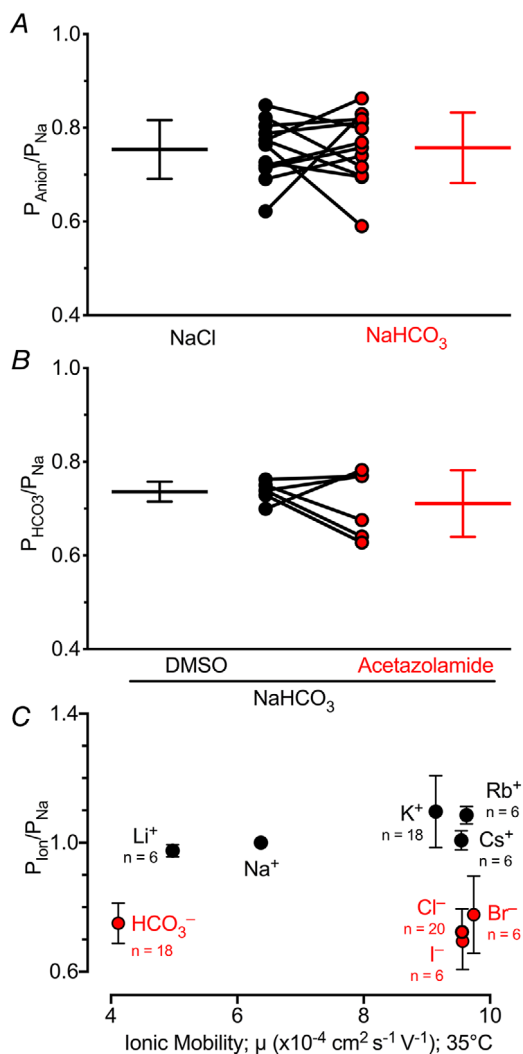


**Figure 2. The paracellular pathway of human airway epithelia is  $\text{HCO}_3^-$  permeable**

$n \geq 6$  donors for all panels and all error bars represent standard deviations of the mean. *A*, paracellular  $P_{\text{Na/Cl}}$  vs.  $P_{\text{Na/HCO}_3}$ , each circle represents a single human donor;  $P = 0.91$ ; two-tailed paired Student's *t* test;  $n = 12$  donors. *B*, paracellular  $P_{\text{Na/HCO}_3} \pm 1 \text{ mM}$  acetazolamide, each circle is one donor;  $P = 0.45$ ; two-tailed paired Student's *t* test;  $n = 6$  donors. *C*, relative paracellular permeabilities,  $P_{\text{ion}}/P_{\text{Na}}$ , for several cations and anions. We cannot reject the null hypothesis that the slopes were zero; cations  $P = 0.15$ , anions  $P = 0.76$ ; *F* test;  $n$  values are shown in figure.

### Proinflammatory cytokines increased ASL pH and eliminated or reversed paracellular $\text{HCO}_3^-$ secretion

Inflammation involves airway epithelia in many lung diseases. Given the importance of ASL pH to respiratory defences, we asked whether cytokines might change the paracellular  $\text{HCO}_3^-$  permeability of airway epithelia and thereby alter ASL pH. IL-13 is a cytokine that is an important mediator of allergic diseases and drives the TH2-high asthma phenotype (Wills-Karp *et al.* 1998; Wesolowska-Andersen & Seibold, 2015; Svenningsen & Nair, 2017). IL-13 may also play an important role in CF (Hauber *et al.* 2003). In a previous study, we applied IL-13 for 21 days to primary cultures of human airway epithelia and induced goblet cell metaplasia (Pezzulo *et al.* 2019). Here we asked whether IL-13 changes paracellular anion permeability and calculated transepithelial  $\text{HCO}_3^-$  fluxes. Compared with the vehicle control, IL-13 increased ASL pH in CF airway epithelia from 6.6 to 7.4 (Table 2). However, IL-13 did not significantly change  $G_p$  or the permeability of  $\text{HCO}_3^-$ ,  $\text{Cl}^-$ ,  $\text{Na}^+$  or  $\text{K}^+$  (Table 2, Fig. 4A). The calculated paracellular  $\text{HCO}_3^-$  conductance increased with the increase in apical  $[\text{HCO}_3^-]$  (Fig. 4B). In vehicle-treated epithelia, we calculated a small secretory  $\text{HCO}_3^-$  flux (Fig. 4C). IL-13 reversed that to a small absorptive  $\text{HCO}_3^-$  flux. These results indicate that the IL-13-induced ASL alkalinization was not likely due to  $\text{HCO}_3^-$  secretion through the paracellular pathway.

We also tested IL-17 and  $\text{TNF}\alpha$  because they are commonly elevated in CF airways. They are involved in neutrophil recruitment (Smart & Casale, 1994; Lukacs *et al.* 1995; Laan *et al.* 1999; Ferretti *et al.* 2003; Stoppelenburg *et al.* 2013; Michel *et al.* 2014), a prominent feature of CF airway disease (Conese *et al.* 2003; Cantin *et al.* 2015; Russell *et al.* 2016; Liu *et al.* 2017). We asked whether these cytokines alter paracellular  $\text{HCO}_3^-$  permeability and  $\text{HCO}_3^-$  secretion and thereby contribute, at least in part, to the increased ASL pH. Compared with the vehicle control, IL-17/ $\text{TNF}\alpha$  increased ASL pH (Table 3). These cytokines increased:  $P_{\text{Na}}$ ,  $P_{\text{Cl}}$  and  $P_{\text{HCO}_3}$  (Table 3, Fig. 4A). However, the increase was not the result of a non-specific leak because they decreased  $P_{\text{Cl/Na}}$  and  $P_{\text{K/Na}}$ , whereas a non-specific leak would be predicted to increase  $P_{\text{Cl/Na}}$  and  $P_{\text{K/Na}}$ . Paracellular  $\text{HCO}_3^-$  conductance increased due to the increased  $P_{\text{HCO}_3}$  and the increased apical  $[\text{HCO}_3^-]$  (Fig. 4B). With vehicle-treated control epithelia, the calculated paracellular  $\text{HCO}_3^-$  flux was small and secretory (Fig. 4C). After IL-17 and  $\text{TNF}\alpha$ , the paracellular  $\text{HCO}_3^-$  flux was not different from zero.

### Discussion

Our results indicate that human airway epithelia have a paracellular pathway that is as permeable to  $\text{HCO}_3^-$  as to  $\text{Cl}^-$ . The  $\text{HCO}_3^-$  permeability indicates that the

paracellular pathway could influence ASL pH. Indeed, under basal conditions, we calculated a small secretory paracellular  $\text{HCO}_3^-$  flux. This flux would tend to counter-balance, in part, the acidic ASL pH produced by  $\text{H}^+$  secretion (Coakley *et al.* 2003; Fischer & Widdicombe, 2006; Shah *et al.* 2016; Lennox *et al.* 2018; Simonin *et al.* 2019). After treating epithelia with the proinflammatory

cytokines, IL-13 and IL-17/TNF $\alpha$ , ASL pH increased. However, at a pH of 7.0, the calculated paracellular  $\text{HCO}_3^-$  fluxes were negligible, and at a pH of 7.4, paracellular  $\text{HCO}_3^-$  fluxes were absorptive. Thus, as the pH of ASL increases towards that of basolateral liquid, paracellular  $\text{HCO}_3^-$  flux becomes absorptive, tempering the alkaline pH generated by transcellular  $\text{HCO}_3^-$  secretion.

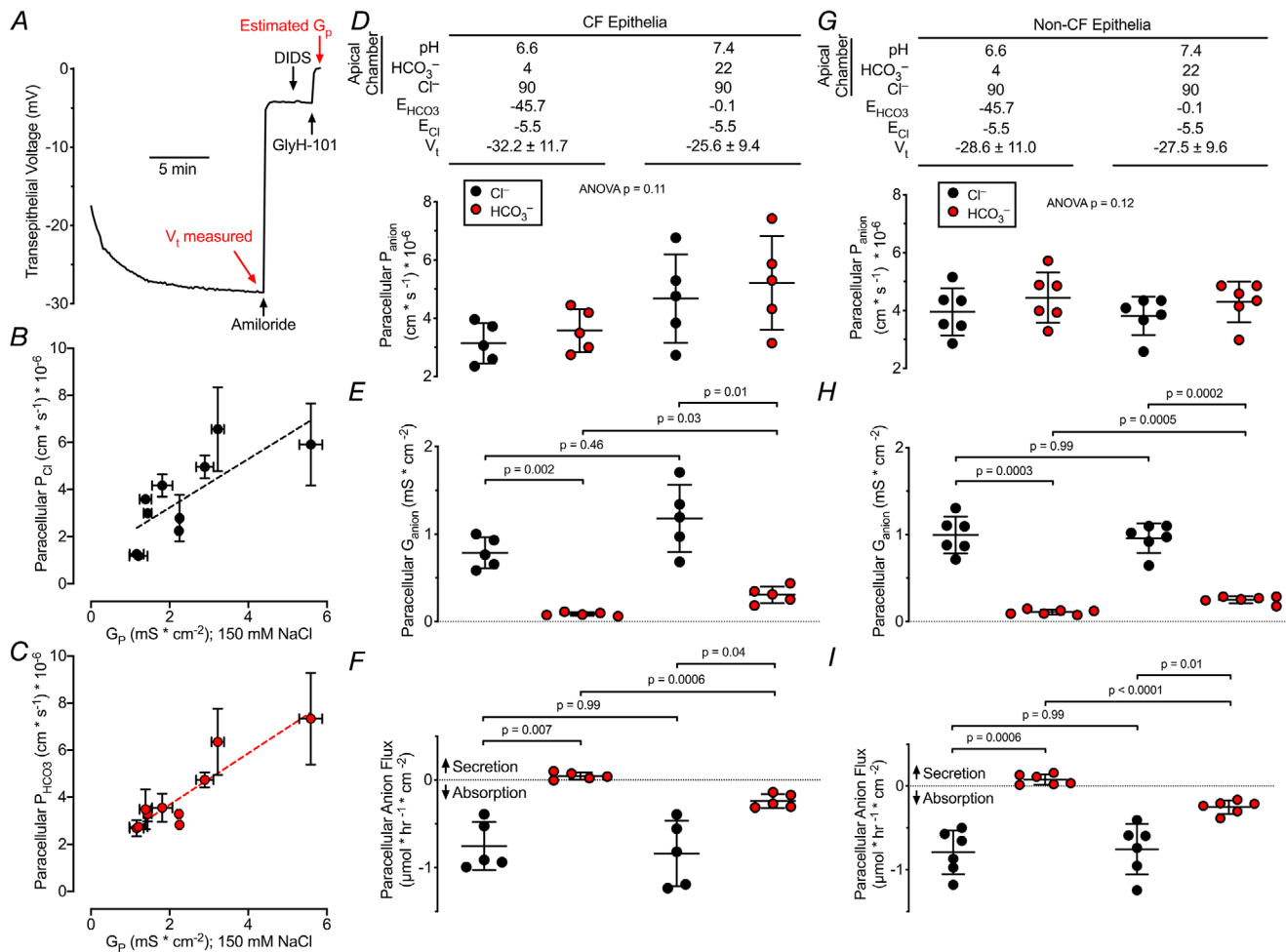


### Figure 3. Human airways have small paracellular $\text{HCO}_3^-$ fluxes

Panels D, E and F;  $n = 5$  cystic fibrosis (CF) donors. 1 of 6 CF donors was excluded from these studies because cultures were unresponsive to amiloride. Black circles represent  $\text{Cl}^-$  data and red circles represent  $\text{HCO}_3^-$  data, each for a single donor. Conditions listed at the top of panel D also apply to aligned data points in panels E and F, and conditions listed at the top of panel G also apply to aligned data points in panels H and I. A, representative transepithelial voltage recording for non-CF epithelia bathed in symmetrical solutions. Non-CF summary data are in panels G–I. The same protocol was performed on CF epithelia to generate subsequent panels. B, paracellular  $P_{\text{Cl}}$  vs. donor-matched 150 mM  $G_p$  from Fig. 1 and 2 data, circles represent 11 donors;  $r^2 = 0.57$ . C, paracellular  $P_{\text{HCO}_3}$  from Fig. 2 data vs. donor-matched 150 mM NaCl  $G_p$  from Fig. 1 and 2 data, circles represent 11 donors;  $r^2 = 0.84$ . D, paracellular  $P_{\text{anion}}$  calculated from  $G_p$  and either Panel B or Panel C; one-way ANOVA. Conditions for groups in panels D–F are shown at top. E,  $G_{\text{anion}}$  calculated using Eqn 6. Paracellular  $G_{\text{HCO}_3}$  increased when apical  $[\text{HCO}_3^-]$  increased; Bonferroni-corrected  $P$  values shown, one-way ANOVA. F, paracellular anion flux calculated using Eqn 9 and Faraday's constant. Minimal paracellular  $\text{HCO}_3^-$  secretion became  $\text{HCO}_3^-$  absorption with increased apical  $[\text{HCO}_3^-]$ ; Bonferroni-corrected  $P$  values shown, one-way ANOVA. G, paracellular  $P_{\text{anion}}$  calculated from  $G_p$  and either Fig. 3B or 3C; one-way ANOVA. H,  $G_{\text{anion}}$  calculated using Eqn 6. Paracellular  $G_{\text{HCO}_3}$  increased when apical  $[\text{HCO}_3^-]$  increased; Bonferroni-corrected  $P$  values shown, one-way ANOVA. I, paracellular anion flux calculated using Eqn 9 and Faraday's constant. Minimal paracellular  $\text{HCO}_3^-$  secretion became  $\text{HCO}_3^-$  absorption with increased apical  $[\text{HCO}_3^-]$ ; Bonferroni-corrected  $P$  values shown, one-way ANOVA.



**Table 2. IL-13 increases airway surface liquid pH of human cystic fibrosis airway epithelia, but does not alter paracellular ion permeabilities**

	21 days vehicle (PBS)	21 days IL-13	P value
Native airway surface liquid (ASL) experiments; <i>n</i> = 6			
ASL pH <sup>†</sup>	6.58; [6.51, 6.63]	7.40; [7.20, 7.76]	<0.0001
22 mM NaCl dilution potential experiments; <i>n</i> = 6			
G <sub>p</sub> (mS cm <sup>-2</sup> )	0.802 ± 0.355	0.755 ± 0.259	0.75
P <sub>Cl/Na</sub>	0.73 ± 0.06	0.61 ± 0.16	0.06
P <sub>Na</sub> (x10 <sup>-6</sup> cm s <sup>-1</sup> )	6.87 ± 2.92	7.08 ± 1.70	0.49
P <sub>Cl</sub> (x10 <sup>-6</sup> cm s <sup>-1</sup> )	5.11 ± 2.39	4.48 ± 2.19	0.15
22 mM NaHCO <sub>3</sub> dilution potential experiments; <i>n</i> = 5 <sup>‡</sup>			
G <sub>p</sub> (mS cm <sup>-2</sup> )	0.664 ± 0.292	0.749 ± 0.158	0.51
P <sub>HCO<sub>3</sub>/Na</sub>	0.74 ± 0.07	0.61 ± 0.18	0.12
P <sub>Na</sub> (x10 <sup>-6</sup> cm s <sup>-1</sup> )	5.44 ± 2.21	6.52 ± 1.57	0.41
P <sub>HCO<sub>3</sub></sub> (x10 <sup>-6</sup> cm s <sup>-1</sup> )	4.43 ± 2.14	4.61 ± 0.85	0.67
150 mM NaCl/KCl bi-ionic potential experiments; <i>n</i> = 5 <sup>‡</sup>			
P <sub>K/Na</sub>	1.09 ± 0.08	1.11 ± 0.12	0.67

Data reported as means ± standard deviation

P values obtained using two-tailed paired Student's *t* test

<sup>†</sup>Statistical analyses, including mean and standard deviation, were performed using [H<sup>+</sup>]. For presentation, the [H<sup>+</sup>] were converted to pH, and hence the standard deviations are shown as intervals.

<sup>‡</sup>Donor excluded from analysis; Grubb's test  $\alpha \leq 0.01$

**Table 3. IL-17/TNF $\alpha$  increases airway surface liquid pH of human cystic fibrosis airway epithelia and alters paracellular ion permeabilities**

	48 h vehicle (PBS)	48 h IL-17/TNF $\alpha$	P value
Native airway surface liquid (ASL) experiments; <i>n</i> = 6			
ASL pH <sup>†</sup>	6.57; [6.54, 6.59]	7.04; [6.93, 7.19]	<0.0001
22 mM NaCl dilution potential experiments; <i>n</i> = 6			
G <sub>p</sub> (mS cm <sup>-2</sup> ) <sup>‡</sup>	0.585 ± 0.158	1.026 ± 0.472	0.03
P <sub>Cl/Na</sub>	0.79 ± 0.04	0.62 ± 0.09	0.01
P <sub>Na</sub> (x10 <sup>-6</sup> cm s <sup>-1</sup> ) <sup>‡</sup>	4.85 ± 1.17	8.90 ± 3.75	0.03
P <sub>Cl</sub> (x10 <sup>-6</sup> cm s <sup>-1</sup> ) <sup>‡</sup>	3.83 ± 0.96	5.61 ± 2.92	0.03
22 mM NaHCO <sub>3</sub> dilution potential experiments; <i>n</i> = 6			
G <sub>p</sub> (mS cm <sup>-2</sup> )	0.597 ± 0.193	1.344 ± 0.390	0.002
P <sub>HCO<sub>3</sub>/Na</sub>	0.74 ± 0.08	0.69 ± 0.05	0.31
P <sub>Na</sub> (x10 <sup>-6</sup> cm s <sup>-1</sup> )	5.06 ± 1.52	11.72 ± 3.07	0.0009
P <sub>HCO<sub>3</sub></sub> (x10 <sup>-6</sup> cm s <sup>-1</sup> )	3.82 ± 1.36	8.23 ± 2.75	0.007
150 mM NaCl/KCl bi-ionic potential experiments; <i>n</i> = 6			
P <sub>K/Na</sub>	1.02 ± 0.04	0.87 ± 0.05	0.005

Data reported as means ± standard deviation

<sup>†</sup>Statistical analyses, including mean and standard deviation, were performed using [H<sup>+</sup>]. For presentation, the [H<sup>+</sup>] were converted to pH, and hence the standard deviations are shown as intervals.

P values obtained using two-tailed paired Student's *t* test or

<sup>‡</sup>Two-tailed Wilcoxon matched-pairs ranked sign

We considered the possibility that inflammation could disrupt the barrier function of airway epithelia. Because ASL has a pH and [HCO<sub>3</sub><sup>-</sup>] that is lower than that of basolateral liquid, barrier disruption might allow basolateral HCO<sub>3</sub><sup>-</sup> to flow into and alkalinize ASL. Both IL-13 and IL-17/TNF $\alpha$  increased ASL pH, whereas IL-13 did not change G<sub>p</sub> or P<sub>HCO<sub>3</sub></sub>, and IL-17/TNF $\alpha$  increased

both. However, both sets of cytokines decreased P<sub>Cl/Na</sub>; the opposite of what would be expected for disruption of the epithelial barrier because the mobility of Cl<sup>-</sup> in water is approximately 1.5 times that of Na<sup>+</sup>. Moreover, pH changes in the physiological range did not alter paracellular conductance or P<sub>Cl/Na</sub>, suggesting that effects of cytokines were not secondary to altered pH.

$\text{HCO}_3^-$  permeated the paracellular pathway as an anion rather than as a  $\text{CO}_2$  reversion reaction as indicated by its carbonic anhydrase insensitivity. Moreover,  $\text{HCO}_3^-$  and other tested monovalent anions had similar permeabilities, and all were approximately 3/4 as permeable as  $\text{Na}^+$ ,  $\text{K}^+$ , and the other tested monovalent cations. It is possible that the size and charge selectivity arose from the summation of many intercellular spaces with distinct size and charge selectivity. However, these data suggest that the net paracellular transport of airway epithelia can be generalized as weakly cation-selective with minimal size selectivity.

Our dilution potential experiments revealed that paracellular  $P_{\text{Cl}}$  and  $P_{\text{HCO}_3^-}$  were equal. A previous report suggested that  $P_{\text{Cl}}$  was greater than  $P_{\text{HCO}_3^-}$  (Coakley *et al.* 2003). A potential explanation for this difference is that the previous study used bi-ionic experiments, and the  $\text{HCO}_3^-$  concentration (125 mM  $\text{HCO}_3^-$ , pH 8.15) might result in

$\text{CO}_3^{2-}$  formation and precipitation of extracellular  $\text{Ca}^{2+}$ , which is required to maintain tight junction integrity (Cerejido *et al.* 1998; Wang *et al.* 2000). Disrupted barrier integrity would lead to an inflated  $P_{\text{Cl}}$  because  $\text{Cl}^-$  has a higher ionic mobility in free solution than  $\text{HCO}_3^-$ . However, other culture or technical differences might be responsible.

The proximal tubule, another epithelium with luminal acidification, has a  $P_{\text{HCO}_3^-}$  that is less than  $P_{\text{Cl}}$  (Cogan & Alpern, 1984). That arrangement may achieve maximal transepithelial  $\text{HCO}_3^-$  absorption as a result of transcellular  $\text{HCO}_3^-$  absorption with minimal  $\text{HCO}_3^-$  reflux through the paracellular pathway, while allowing paracellular  $\text{Cl}^-$  absorption. The factors that determine the ratio of  $P_{\text{HCO}_3^-}$  to  $P_{\text{Cl}}$  in the proximal tubule or in airway epithelia are unknown. However, it may be relevant that absolute paracellular permeabilities in the proximal tubule are much greater than in airway epithelia.

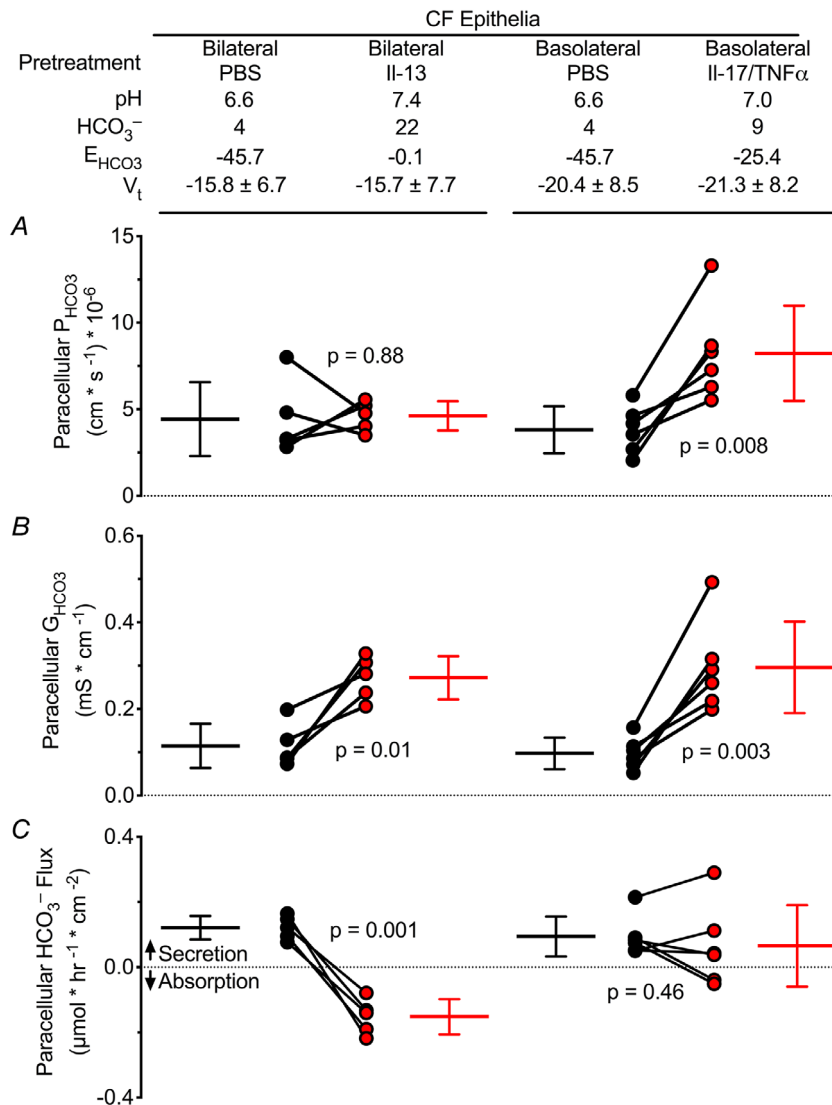


**Figure 4.** Proinflammatory cytokines increased airway surface liquid pH and induce  $\text{HCO}_3^-$  absorption or minimal  $\text{HCO}_3^-$  flux

1 of 6 cystic fibrosis (CF) donors was excluded from the IL-13 analysis because of a high IL-13-induced paracellular  $\text{HCO}_3^-$  conductance of  $0.868 \text{ mS cm}^{-2}$ , Grubb's test  $\alpha \leq 0.01$ . Red circles represent  $\text{HCO}_3^-$  data and black circles represent  $\text{Cl}^-$  data, each for a single donor. **A**, paracellular  $P_{\text{HCO}_3^-}$  reported in Table 2 and Table 3; two-tailed paired Student's  $t$  test,  $P$  values shown. **B**,  $G_{\text{HCO}_3^-}$  calculated using Eqn 6, paracellular  $G_{\text{HCO}_3^-}$  increased due to increased apical  $[\text{HCO}_3^-]$ ; two-tailed paired Student's  $t$  test,  $P$  values shown. **C**, paracellular  $\text{HCO}_3^-$  flux calculated using Eqn 9 and Faraday's constant. Minimal  $\text{HCO}_3^-$  secretion was reduced or absorptive with cytokine treatments; two-tailed paired Student's  $t$  test,  $P$  values shown.

Previous studies have reported that IL-13 increased (Lennox *et al.* 2018) and decreased (Haggie *et al.* 2016) ASL pH. Applying IL-17 to airway epithelia for two days was also reported to increase ASL pH (Kreindler *et al.* 2009). We found that treating epithelia for 21 days with IL-13 or two days with IL-17/TNF $\alpha$  increased ASL pH. Interestingly, IL-13 did not alter G<sub>p</sub>, and in a separate study, one day of IL-17/TNF $\alpha$  treatment increased ASL pH but did not alter G<sub>p</sub> (Rehman *et al.* 2020). These differences highlight the likely contribution of time of treatment and identity of cytokine for responses, as has been previously noted (Coyne *et al.* 2002). In addition to cytokines, second messengers might alter paracellular HCO<sub>3</sub><sup>-</sup> flux. Previous reports with differentiated airway cell lines suggested that cAMP alters the paracellular conductance (Nilsson *et al.* 2010; Weiser *et al.* 2011). Whether or not HCO<sub>3</sub><sup>-</sup> flux is appreciable under these conditions will depend on P<sub>HCO<sub>3</sub><sup>-</sup></sub>, V<sub>t</sub>, and the apical pH after cAMP stimulation.

Our study has limitations. We used the Goldman–Hodgkin–Katz equation, which assumes a constant electrical field, to obtain ion permeabilities. It is possible that along the lateral space the ion encounters more complex forces than a constant field. We did not consider the unstirred layer effect, which was likely nominal because the osmotic-induced water permeability of airway epithelia is independent of bath perfusion rates (Folkesson *et al.* 1996). We did not address paracellular proton permeability, which cannot be measured by electrophysiological methods due to its nanomolar concentration. However, the lumen-negative trans-epithelial voltages of airway epithelia predict paracellular proton secretion with inflammatory cytokines, which are not consistent with the alkalinization observed. We performed dilution potential experiments with CF airway epithelia to reduce transcellular Cl<sup>-</sup> and HCO<sub>3</sub><sup>-</sup> secretion and extended the permeability values to non-CF airways. However, LeSimple *et al.* (LeSimple *et al.* 2010) found that CFTR expression in immortalized CF epithelial cells increased transepithelial resistance via tight junction assembly. Li *et al.* (2012) found that CFTR expression in MDCK cells decreased transepithelial resistance. Consistent with a role for CFTR in tight junction assembly, Ruan *et al.* (2014) found that CFTR co-localizes with ZO-1 in the trachea. However, our estimated G<sub>p</sub> was similar for CF and non-CF epithelia.

These data suggest that the paracellular pathway acts as a HCO<sub>3</sub><sup>-</sup> shunt. Under physiological conditions, the reversal potential for HCO<sub>3</sub><sup>-</sup> is slightly hyperpolarized relative to V<sub>t</sub> and passive HCO<sub>3</sub><sup>-</sup> flux through the paracellular pathway opposes net transepithelial acidification. Under pathological conditions that increase the ASL pH, such as those modelled by cytokine treatment, the reversal potential for HCO<sub>3</sub><sup>-</sup> is depolarized relative to the V<sub>t</sub> and passive HCO<sub>3</sub><sup>-</sup> flux opposes net transepithelial alkalinization. This shunting mechanism may

help to maintain an optimal ASL pH for antimicrobial activity and mucus rheology.

## References

- Abou Alaiwa M, Launspach J, Grogan B, Carter S, Zabner J, Stoltz DA, Singh PK, McKone EF & Welsh MJ (2018). Ivacaftor-induced sweat chloride reductions correlate with increases in airway surface liquid pH in cystic fibrosis. *JCI Insight* **3**, pii: 121468.
- Abou Alaiwa MH, Beer AM, Pezzulo AA, Launspach JL, Horan RA, Stoltz DA, Starner TD, Welsh MJ & Zabner J (2014a). Neonates with cystic fibrosis have a reduced nasal liquid pH; A small pilot study. *J Cyst Fibros* **13**, 373–377.
- Abou Alaiwa MH, Reznikov LR, Gansemer ND, Sheets KA, Horswill AR, Stoltz DA, Zabner J & Welsh MJ (2014b). pH modulates the activity and synergism of the airway surface liquid antimicrobials beta-defensin-3 and LL-37. *Proc Natl Acad Sci U S A* **111**, 18703–18708.
- Anderson JM & Van Itallie CM (2009). Physiology and function of the tight junction. *Cold Spring Harb Perspect Biol* **1**, a002584.
- Atherton HC, Jones G & Danahay H (2003). IL-13-induced changes in the goblet cell density of human bronchial epithelial cell cultures: MAP kinase and phosphatidylinositol 3-kinase regulation. *Am J Physiol Lung Cell Mol Physiol* **285**, L730–L739.
- Cantin AM, Hartl D, Konstan MW & Chmiel JF (2015). Inflammation in cystic fibrosis lung disease: pathogenesis and therapy. *J Cyst Fibros* **14**, 419–430.
- Cerejido M, Valdes J, Shoshani L & Contreras RG (1998). Role of tight junctions in establishing and maintaining cell polarity. *Annu Rev Physiol* **60**, 161–177.
- Choy DF, Hart KM, Borthwick LA, Shikotra A, Nagarkar DR, Siddiqui S, Jia G, Ohri CM, Doran E, Vannella KM, Butler CA, Hargadon B, Sciruba JC, Gieseck RL, Thompson RW, White S, Abbas AR, Jackman J, Wu LC, Egen JG, Heaney LG, Ramalingam TR, Arron JR, Wynn TA & Bradding P (2015). TH2 and TH17 inflammatory pathways are reciprocally regulated in asthma. *Sci Transl Med* **7**, 301ra129.
- Clary-Meinesz C, Mouroux J, Cosson J, Huitorel P & Blaive B (1998). Influence of external pH on ciliary beat frequency in human bronchi and bronchioles. *Eur Respir J* **11**, 330–333.
- Coakley RD, Grubb BR, Paradiso AM, Gatzky JT, Johnson LG, Kreda SM, O'Neal WK & Boucher RC (2003). Abnormal surface liquid pH regulation by cultured cystic fibrosis bronchial epithelium. *Proc Natl Acad Sci U S A* **100**, 16083–16088.
- Cogan MG & Alpern RJ (1984). Regulation of proximal bicarbonate reabsorption. *Am J Physiol* **247**, F387–F395.
- Conese M, Copreni E, Di Gioia S, De Rinaldis P & Fumarulo R (2003). Neutrophil recruitment and airway epithelial cell involvement in chronic cystic fibrosis lung disease. *J Cyst Fibros* **2**, 129–135.
- Coyne CB, Vanhook MK, Gambling TM, Carson JL, Boucher RC & Johnson LG (2002). Regulation of airway tight junctions by proinflammatory cytokines. *Mol Biol Cell* **13**, 3218–3234.

- Dakin CJ, Numa AH, Wang H, Morton JR, Vertzyas CC & Henry RL (2002). Inflammation, infection, and pulmonary function in infants and young children with cystic fibrosis. *Am J Respir Crit Care Med* **165**, 904–910.
- Diamond JM (1978). Channels in epithelial cell membranes and junctions. *Fed Proc* **37**, 2639–2643.
- Dickinson JD, Alevy Y, Malvin NP, Patel KK, Gunsten SP, Holtzman MJ, Stappenbeck TS & Brody SL (2016). IL13 activates autophagy to regulate secretion in airway epithelial cells. *Autophagy* **12**, 397–409.
- Faul F, Erdfelder E, Lang AG & Buchner A (2007). G\*Power 3: a flexible statistical power analysis program for the social, behavioral, and biomedical sciences. *Behav Res Methods* **39**, 175–191.
- Ferretti S, Bonneau O, Dubois GR, Jones CE & Trifilieff A (2003). IL-17, produced by lymphocytes and neutrophils, is necessary for lipopolysaccharide-induced airway neutrophilia: IL-15 as a possible trigger. *J Immunol* **170**, 2106–2112.
- Fischer H & Widdicombe JH (2006). Mechanisms of acid and base secretion by the airway epithelium. *J Membr Biol* **211**, 139–150.
- Folkesson HG, Matthay MA, Frigeri A & Verkman AS (1996). Transepithelial water permeability in microperfused distal airways. Evidence for channel-mediated water transport. *J Clin Invest* **97**, 664–671.
- Garland AL, Walton WG, Coakley RD, Tan CD, Gilmore RC, Hobbs CA, Tripathy A, Clunes LA, Bencharit S, Stutts MJ, Betts L, Redinbo MR & Tarran R (2013). Molecular basis for pH-dependent mucosal dehydration in cystic fibrosis airways. *Proc Natl Acad Sci U S A* **110**, 15973–15978.
- Garnett JP, Kalsi KK, Sobotta M, Bearham J, Carr G, Powell J, Brodrie M, Ward C, Tarran R & Baines DL (2016). Hyperglycaemia and pseudomonas aeruginosa acidify cystic fibrosis airway surface liquid by elevating epithelial monocarboxylate transporter 2 dependent lactate-H(+) secretion. *Sci Rep* **6**, 37955.
- Goldman DE (1943). Potential, impedance, and rectification in membranes. *J Gen Physiol* **27**, 37–60.
- Gorrieri G, Scudieri P, Caci E, Schiavon M, Tomati V, Sirci F, Napolitano F, Carrella D, Gianotti A, Musante I, Favia M, Casavola V, Guerra L, Rea F, Ravazzolo R, Di Bernardo D & Galletta LJ (2016). Goblet cell hyperplasia requires high bicarbonate transport to support mucin release. *Sci Rep* **6**, 36016.
- Grundy D (2015). Principles and standards for reporting animal experiments in The Journal of Physiology and Experimental Physiology. *J Physiol* **593**, 2547–2549.
- Haggie PM, Phuan PW, Tan JA, Zlock L, Finkbeiner WE & Verkman AS (2016). Inhibitors of pendrin anion exchange identified in a small molecule screen increase airway surface liquid volume in cystic fibrosis. *FASEB J* **30**, 2187–2197.
- Hastings AB & Sendroy JJ (1925). The effect of variation in ionic strength on the apparent first and second dissociation constants of carbonic acid. *J Biol Chem* **65**, 445–455.
- Hauber HP, Gholami D, Koppermann G, Heuer HE, Meyer A & Pforte A (2003). Increased expression of interleukin-13 but not interleukin-4 in cystic fibrosis patients. *J Cyst Fibros* **2**, 189–194.
- Hodgkin AL & Katz B (1949). The effect of sodium ions on the electrical activity of giant axon of the squid. *J Physiol* **108**, 37–77.
- Hoegger MJ, Fischer AJ, McMenimen JD, Ostedgaard LS, Tucker AJ, Awadalla MA, Moninger TO, Michalski AS, Hoffman EA, Zabner J, Stoltz DA & Welsh MJ (2014). Impaired mucus detachment disrupts mucociliary transport in a piglet model of cystic fibrosis. *Science* **345**, 818–822.
- Jayaraman S, Song Y & Verkman AS (2001a). Airway surface liquid pH in well-differentiated airway epithelial cell cultures and mouse trachea. *Am J Physiol* **281**, C1504–C1511.
- Jayaraman S, Song Y, Vetrivel L, Shankar L & Verkman AS (2001b). Noninvasive *in vivo* fluorescence measurement of airway surface liquid depth, salt concentration, and pH. *J Clin Invest* **107**, 317–324.
- Kanoh S, Tanabe T & Rubin BK (2011). IL-13-induced MUC5AC production and goblet cell differentiation is steroid resistant in human airway cells. *Clin Exp Allergy* **41**, 1747–1756.
- Kao CY, Chen Y, Thai P, Wachi S, Huang F, Kim C, Harper RW & Wu R (2004). IL-17 markedly up-regulates beta-defensin-2 expression in human airway epithelium via JAK and NF-kappaB signaling pathways. *J Immunol* **173**, 3482–3491.
- Karp PH, Moninger T, Weber SP, Nesselhauf TS, Launsbach J, Zabner J & Welsh MJ (2002). An *in vitro* model of differentiated human airway epithelia: methods and evaluation of primary cultures. In *Epithelial Cell Culture Protocols*, ed. Wise C, pp. 115–137. Humana Press, Inc., Totowa, NJ.
- Khan TZ, Wagener JS, Bost T, Martinez J, Accurso FJ & Riches DW (1995). Early pulmonary inflammation in infants with cystic fibrosis. *Am J Respir Crit Care Med* **151**, 1075–1082.
- Kielland J (1937). Individual activity coefficients of ions in aqueous solutions. *J Am Chem Soc* **59**, 1675–1678.
- Kim D, Huang J, Billet A, Abu-Arish A, Goepf J, Matthes E, Tewfik MA, Frenkiel S & Hanrahan JW (2019). Pendrin mediates bicarbonate secretion and enhances CFTR function in airway surface epithelia. *Am J Respir Cell Mol Biol* **60**, 705–716.
- Kimizuka H & Koketsu K (1964). Ion transport through cell membrane. *J Theor Biol* **6**, 290–305.
- Knowles MR, Robinson JM, Wood RE, Pue CA, Mentz WM, Wager GC, Gatzky JT & Boucher RC (1997). Ion composition of airway surface liquid of patients with cystic fibrosis as compared with normal and disease-control subjects. *J Clin Invest* **100**, 2588–2595.
- Kreindler JL, Bertrand CA, Lee RJ, Karasic T, Aujla S, Pilewski JM, Frizzell RA & Kolls JK (2009). Interleukin-17A induces bicarbonate secretion in normal human bronchial epithelial cells. *Am J Physiol Lung Cell Mol Physiol* **296**, L257–266.
- Laan M, Cui ZH, Hoshino H, Lotvall J, Sjostrand M, Gruenert DC, Skoogh BE & Linden A (1999). Neutrophil recruitment by human IL-17 via C-X-C chemokine release in the airways. *J Immunol* **162**, 2347–2352.
- Laoukili J, Perret E, Willems T, Minty A, Parthoens E, Houcine O, Coste A, Jorissen M, Marano F, Caput D & Tournier F (2001). IL-13 alters mucociliary differentiation and ciliary beating of human respiratory epithelial cells. *J Clin Invest* **108**, 1817–1824.



- Lehmann R, Muller MM, Klassert TE, Driesch D, Stock M, Heinrich A, Conrad T, Moore C, Schier UK, Guthke R & Slevogt H (2018). Differential regulation of the transcriptomic and secretomic landscape of sensor and effector functions of human airway epithelial cells. *Mucosal Immunol* **11**, 627–642.
- Lennox AT, Coburn SL, Leech JA, Heidrich EM, Kleyman TR, Wenzel SE, Pilewski JM, Corcoran TE & Myerburg MM (2018). ATP12A promotes mucus dysfunction during type 2 airway inflammation. *Sci Rep* **8**, 2109.
- LeSimple P, Liao J, Robert R, Gruenert DC & Hanrahan JW (2010). Cystic fibrosis transmembrane conductance regulator trafficking modulates the barrier function of airway epithelial cell monolayers. *J Physiol* **588**, 1195–1209.
- Li H, Yang W, Mendes F, Amaral MD & Sheppard DN (2012). Impact of the cystic fibrosis mutation F508del-CFTR on renal cyst formation and growth. *Am J Physiol Renal Physiol* **303**, F1176–F1186.
- Liu J, Pang Z, Wang G, Guan X, Fang K, Wang Z & Wang F (2017). Advanced role of neutrophils in common respiratory diseases. *J Immunol Res* **2017**, 6710278.
- Lukacs NW, Strieter RM, Chensue SW, Widmer M & Kunkel SL (1995). TNF- $\alpha$  mediates recruitment of neutrophils and eosinophils during airway inflammation. *J Immunol* **154**, 5411–5417.
- Manov GG, Bates RG, Hamer WJ & Acree SF (1943). Values of the constants in the Debye—Hückel equation for activity coefficients. *J Am Chem Soc* **65**, 1765–1767.
- McAllister F, Henry A, Kreindler JL, Dubin PJ, Ulrich L, Steele C, Finder JD, Pilewski JM, Carreno BM, Goldman SJ, Pirhonen J & Kolls JK (2005). Role of IL-17A, IL-17E, and the IL-17 receptor in regulating growth-related oncogene- $\alpha$  and granulocyte colony-stimulating factor in bronchial epithelium: implications for airway inflammation in cystic fibrosis. *J Immunol* **175**, 404–412.
- McShane D, Davies JC, Davies MG, Bush A, Geddes DM & Alton EW (2003). Airway surface pH in subjects with cystic fibrosis. *Eur Respir J* **21**, 37–42.
- Michel O, Dinh PH, Doyen V & Corazza F (2014). Anti-TNF inhibits the airways neutrophilic inflammation induced by inhaled endotoxin in human. *BMC Pharmacol Toxicol* **15**, 60.
- Muhlebach MS, Stewart PW, Leigh MW & Noah TL (1999). Quantitation of inflammatory responses to bacteria in young cystic fibrosis and control patients. *Am J Respir Crit Care Med* **160**, 186–191.
- Namkung W, Song Y, Mills AD, Padmawar P, Finkbeiner WE & Verkman AS (2009). In situ measurement of airway surface liquid [K<sup>+</sup>] using a ratioable K<sup>+</sup>-sensitive fluorescent dye. *J Biol Chem* **284**, 15916–15926.
- Nilsson HE, Dragomir A, Lazorova L, Johannesson M & Roomans GM (2010). CFTR and tight junctions in cultured bronchial epithelial cells. *Exp Mol Pathol* **88**, 118–127.
- Ostedgaard LS, Moninger TO, McMenimen JD, Sawin NM, Parker CP, Thornell IM, Powers LS, Gansemer ND, Bouzek DC, Cook DP, Meyerholz DK, Abou Alaiwa MH, Stoltz DA & Welsh MJ (2017). Gel-forming mucins form distinct morphologic structures in airways. *Proc Natl Acad Sci U S A* **114**, 6842–6847.
- Ousingsawat J, Martins JR, Schreiber R, Rock JR, Harfe BD & Kunzelmann K (2009). Loss of TMEM16A causes a defect in epithelial Ca<sup>2+</sup>-dependent chloride transport. *J Biol Chem* **284**, 28698–28703.
- Pezzulo AA, Tang XX, Hoegger MJ, Alaiwa MH, Ramachandran S, Moninger TO, Karp PH, Wohlford-Lenane CL, Haagsman HP, van Eijk M, Banfi B, Horswill AR, Stoltz DA, McCray PB, Jr., Welsh MJ & Zabner J (2012). Reduced airway surface pH impairs bacterial killing in the porcine cystic fibrosis lung. *Nature* **487**, 109–113.
- Pezzulo AA, Tudas RA, Stewart CG, Buonfiglio LGV, Lindsay BD, Taft PJ, Gansemer ND & Zabner J (2019). HSP90 inhibitor geldanamycin reverts IL-13- and IL-17-induced airway goblet cell metaplasia. *J Clin Invest* **129**, 744–758.
- Rehman T, Thornell IM, Pezzulo AA, Thurman AL, Romano Ibarra GS, Karp PH, Tan P, Duffey ME & Welsh MJ (2020). TNF $\alpha$  and IL-17 alkalize airway surface liquid through CFTR and pendrin. *Am J Physiol Cell Physiol*.
- Robinson RA & Stokes RH (1959). Electrolyte solutions: the measurement and interpretation of conductance, chemical potential, and diffusion in solutions of simple electrolytes.
- Ruan YC, Wang Y, Da Silva N, Kim B, Diao RY, Hill E, Brown D, Chan HC & Breton S (2014). CFTR interacts with ZO-1 to regulate tight junction assembly and epithelial differentiation through the ZONAB pathway. *J Cell Sci* **127**, 4396–4408.
- Russell DW, Gaggari A & Solomon GM (2016). Neutrophil fates in bronchiectasis and  $\alpha$ -1 antitrypsin deficiency. *Ann Am Thorac Soc* **13**(Suppl 2), S123–S129.
- Schultz A, Puvvadi R, Borisov SM, Shaw NC, Klimant I, Berry LJ, Montgomery ST, Nguyen T, Kreda SM, Kicic A, Noble PB, Button B & Stick SM (2017). Airway surface liquid pH is not acidic in children with cystic fibrosis. *Nat Commun* **8**, 1409.
- Schultz SG (1980). *Basic Principles of Membrane Transport*. Cambridge University Press, Cambridge.
- Scudieri P, Musante I, Caci E, Venturini A, Morelli P, Walter C, Tosi D, Palleschi A, Martin-Vasallo P, Sermet-Gaudelus I, Planelles G, Crambert G & Galietta LJ (2018). Increased expression of ATP12A proton pump in cystic fibrosis airways. *JCI Insight* **3**, e123616.
- Shah VS, Meyerholz DK, Tang XX, Reznikov L, Abou Alaiwa M, Ernst SE, Karp PH, Wohlford-Lenane CL, Heilmann KP, Leidinger MR, Allen PD, Zabner J, McCray PBJ, Ostedgaard LS, Stoltz DA, Randak CO & Welsh MJ (2016). Airway acidification initiates host defense abnormalities in cystic fibrosis mice. *Science* **351**, 503–507.
- Simonin J, Bille E, Crambert G, Noel S, Dreano E, Edwards A, Hatton A, Pranke I, Villeret B, Cottart CH, Vrel JP, Urbach V, Baatallah N, Hinzpeter A, Golec A, Touqui L, Nassif X, Galietta LJV, Planelles G, Sallenave JM, Edelman A & Sermet-Gaudelus I (2019). Airway surface liquid acidification initiates host defense abnormalities in cystic fibrosis. *Sci Rep* **9**, 6516.
- Sly PD, Brennan S, Gangell C, de Klerk N, Murray C, Mott L, Stick SM, Robinson PJ, Robertson CF & Ranganathan SC (2009). Lung disease at diagnosis in infants with cystic fibrosis detected by newborn screening. *Am J Respir Crit Care Med* **180**, 146–152.

- Smart SJ & Casale TB (1994). Pulmonary epithelial cells facilitate TNF- $\alpha$ -induced neutrophil chemotaxis. A role for cytokine networking. *J Immunol* **152**, 4087–4094.
- Sten-Knudsen O (2002). *Biological Membranes: Theory of Transport, Potentials and Electric Impulses*. Cambridge University Press, Cambridge.
- Stoppelenburg AJ, Salimi V, Hennus M, Plantinga M, Huis in 't Veld R, Walk J, Meering J, Coenjaerts F, Bont L & Boes M (2013). Local IL-17A potentiates early neutrophil recruitment to the respiratory tract during severe RSV infection. *PLoS One* **8**, e78461.
- Svenningsen S & Nair P (2017). Asthma endotypes and an overview of targeted therapy for asthma. *Front Med (Lausanne)* **4**, 158.
- Tang XX, Ostedgaard LS, Hoegger MJ, Moninger TO, Karp PH, McMenimen JD, Choudhury B, Varki A, Stoltz DA & Welsh MJ (2016). Acidic pH increases airway surface liquid viscosity in cystic fibrosis. *J Clin Invest* **126**, 879–891.
- Thavagnanam S, Parker JC, McBrien ME, Skibinski G, Heaney LG & Shields MD (2011). Effects of IL-13 on mucociliary differentiation of pediatric asthmatic bronchial epithelial cells. *Pediatr Res* **69**, 95–100.
- Thornell IM, Rehman T & Welsh MJ (2019a). Inflammatory cytokines IL-13 or IL-17/TNF $\alpha$  do not alter the low paracellular bicarbonate permeability of cystic fibrosis airway epithelia. *FASEB J* **33**, 544.15–544.15.
- Thornell IM, Rehman T & Welsh MJ (2019b). Paracellular bicarbonate flux is minimal in human cystic fibrosis airway epithelia. *Pediatr Pulmonol* **54**, S164–S164.
- Van Slyke DD, Sendroy JJ, Hastings AB & Neill JM (1928). Studies of gas and electrolyte equilibria in blood: X. the solubility of carbon dioxide at 38° in water, salt solution, serum, and blood cells. *J Biol Chem* **78**, 765–799.
- Voipio J (1998). Diffusion and buffering aspects of H<sup>+</sup>, HCO<sub>3</sub><sup>-</sup>, and CO<sub>2</sub> movements in brain tissue. In *pH and Brain Function*, ed. Kaila K & Ranson BR, pp. 45–66. Wiley-Liss, New York.
- Wang G, Zabner J, Deering C, Launspach J, Shao J, Bodner M, Jolly DJ, Davidson BL & McCray PB, Jr (2000). Increasing epithelial junction permeability enhances gene transfer to airway epithelia *in vivo*. *Am J Respir Cell Mol Biol* **22**, 129–138.
- Weiser N, Molenda N, Urbanova K, Bahler M, Pieper U, Oberleithner H & Schillers H (2011). Paracellular permeability of bronchial epithelium is controlled by CFTR. *Cell Physiol Biochem* **28**, 289–296.
- Wesolowska-Andersen A & Seibold MA (2015). Airway molecular endotypes of asthma: dissecting the heterogeneity. *Curr Opin Allergy Clin Immunol* **15**, 163–168.
- Wills-Karp M, Luyimbazi J, Xu X, Schofield B, Neben TY, Karp CL & Donaldson DD (1998). Interleukin-13: central mediator of allergic asthma. *Science* **282**, 2258–2261.
- Zhen G, Park SW, Nguyenvu LT, Rodriguez MW, Barbeau R, Paquet AC & Erle DJ (2007). IL-13 and epidermal growth factor receptor have critical but distinct roles in epithelial cell mucin production. *Am J Respir Cell Mol Biol* **36**, 244–253.

## Additional information

### Author contributions

IMT, TR, AAP and MJW conceived and designed the studies. IMT, TR and AAP conducted the experiments and acquired the data. IMT, TR, AAP and MJW analysed the data. IMT and MJW wrote the manuscript. All authors revised the manuscript.

### Competing interests

No conflicts of interest, financial or otherwise, are declared by the authors.

### Funding

This work was supported by the National Institutes of Health (HL007638) to IMT, HL140261 to AAP, (HL051670 and HL091842) to MJW, and a Cystic Fibrosis Foundation Research Development Program pilot award to TR. IMT is supported by the Gilead Sciences Research Program in Cystic Fibrosis. AAP is supported by the Parker B. Francis Fellowship Program. MJW is an investigator of the Howard Hughes Medical Institute.

### Acknowledgements

GlyH-101 was a generous gift from the Cystic Fibrosis Foundation Therapeutics and Robert Bridges. We thank the University of Iowa In Vitro Models and Cell Culture Core for their technical assistance. Portions of this work have been published in preliminary form (Thornell *et al.* 2019a, b).

### Keywords

airway, bicarbonate, epithelia, ion transport

### Supporting information

Additional supporting information may be found online in the Supporting Information section at the end of the article.

### Statistical Summary Document